Int. J. Heat Mass Transfer. Vol. 15, pp. 1585–1602. Pergamon Press 1972. Printed in Great Britain

EXPERIMENTAL FRICTION FACTORS FOR TURBULENT FLOW WITH SUCTION IN A POROUS TUBE

J. K. AGGARWAL,* M. A. HOLLINGSWORTH and Y. R. MAYHEW
Department of Mechanical Engineering, University of Bristol, Bristol, England

(*Received* 15 *June* 1971 *and in revised form* 1 *October* 1971)

Abstract—Measurements of pressure gradient have been obtained with air flowing in a porous tube of circular cross-section with fully-developed turbulent profile at the entrance and with uniform mass extraction through the wall; an empirical correlation for the axial gradients with suction is presented. A slight but insignificant gradient in the radial direction was detected. The experiments covered an inlet Reynolds number range of 11 000–101 000 with a ratio of the transverse velocity at the wall to the mean axial velocity at inlet from zero to about 0·027. The radial distributions of both the temporal-mean axial velocity and the absolute turbulent velocity fluctuation were measured at the tube exit and the velocity profile parameter has been correlated with a suction parameter. The form of the temporal-mean velocity profile is found to depend critically upon the suction rate, becoming more flat at modest rates of suction but more peaked at high rates. The relative turbulence level is found to increase with suction at all radii, save for some reduction in the region of the wall at very low rates of suction.

Local and average values of the effective friction factor with suction have been computed and are presented in graphical form. At a fixed inlet Reynolds number average values increased markedly with suction but decreased along the tube. For a given local Reynolds number local values displayed a similar trend.

NOMENCLATURE

A_p, area occupied by pores;
A_s, effective surface area;
D, inside diameter of porous tube,
f_0, friction factor without suction $[=\tau_{w0}/\frac{1}{2}\rho\bar{u}^2]$;
f_e, local effective friction factor $[=\tau_{we}/\frac{1}{2}\rho\bar{u}^2]$;
$\bar{f}_e$, average effective friction factor $[=\bar{\tau}_{we}/\frac{1}{2}\rho\bar{u}_1^2]$;
K_{1-6}, coefficients as used in equation (22);
k, average 'Talysurf' roughness of tube inner surface;
k_s, equivalent sand roughness;
L, length of porous tube;
m, axial mass flow rate;
p, static pressure;
R, inside radius of porous tube;
Re_D, Reynolds number $[=\rho\bar{u}D/\mu]$;
r, radial distance from tube axis;
$\bar{r}$, non-dimensional radial distance $[=r/R]$;
u, temporal-mean axial velocity;
$\bar{u}, \bar{u}^2$, area averages over tube cross-section of axial velocity and velocity squared;
u_{max}, temporal-mean maximum axial velocity;
u', axial turbulent velocity fluctuation;
v, temporal-mean radial velocity;
v', radial turbulent velocity fluctuation;
x, axial distance from entry of porous tube;
$\bar{x}$, non-dimensional distance $[=x/L]$;
α, fractional mass extraction parameter [defined by equation (2)];
β, suction coefficient $[=v_w/\bar{u}]$;
δ, velocity profile parameter [defined by equation (9)];
μ, dynamic viscosity of fluid;
ν, kinematic viscosity of fluid $[=\mu/\rho]$;
Π, pressure coefficient [defined by equation (15)];
ρ, fluid density;
τ_w, viscous wall shear stress $[=-\mu(\partial u/\partial r)_w]$;
τ_{w0}, wall shear stress without suction;

* Now at Dept. of Engineering Science, Parks Road, University of Oxford, Oxford.

τ_{we}, local value of effective wall shear stress [defined by equation (4)];
$\bar{\tau}_{we}$, average value of effective wall shear stress [defined by equation (18)];
Ψ, momentum loss coefficient [defined by equation (25)].

Subscripts

1, at inlet to porous tube;
2, at outlet from porous tube;
CW, based on Colebrook–White friction law;
w, at the effective surface of porous tube.

1. INTRODUCTION

THE TEMPERATURE of the gases in the neighbourhood of certain elements of turbojets and rockets (e.g. turbine blades, combustion chambers, exhaust nozzles) has increased faster than the development of new materials capable of withstanding such a temperature whilst maintaining their strength properties. This has directed attention towards methods of cooling existing materials so that the surface temperature can be kept down to the metallurgically accepted limit. A particularly relevant example is that of the turbine blades of modern aircraft engines, which are currently cooled by the passage of relatively cool air tapped from the compressor, either through hollow blades or through spanwise holes drilled in solid blades. Blades which utilize a limited amount of film-cooling in addition to internal convective cooling, by passing the bled air to the outer surfaces of the blades through small holes, are also used.

In the recent past there have been great advances in the methods of manufacturing porous materials, and these advances have reawakened interest in transpiration cooling [1–3], in which a poorly conducting cold fluid is passed through a porous material in a direction opposite to the direction of heat flow; the presence of a thin layer of relatively cool fluid thus maintained between the surface to be cooled and the high-temperature fluid stream adjacent to it reduces the heat transfer coefficient on the hot side. That the technique of transpiration cooling can be very effective was demonstrated as early as the late 1940's [4, 5], and interest has recently been focused upon transpiration-cooled turbine blades. Bayley and Turner [2] have studied the heat transfer performance of a cascade of porous blades in some detail, principally concerning themselves with the outer surface heat transfer coefficient and the conduction through the porous material. In order to compute the overall heat transfer coefficient, however, a knowledge of the inner surface heat transfer coefficient is necessary; values for this coefficient are not known, and work on this topic is currently in progress and will be reported in a later paper.

Values for the friction factors associated with flow in tubes having porous walls are also unknown, at least at high suction rates. These values will be required for assessing the power requirements for this form of cooling and also for any analogy that may be established between heat transfer and wall shear stress under suction conditions. Furthermore there is an analogy between this type of flow and that of a condensing vapour, so that the friction factor with suction may provide a useful indication of the drag between a flowing vapour and its own condensate film. Hitherto, no direct measurements have been made of friction factors at the relatively high suction rates that correspond to fairly common rates of condensation.

The aim of the research reported herein was to determine experimentally local and average friction factors over a large range of suction rates, and in order to simplify the conditions, the suction rate was kept uniform along the tube and the flow was fully developed at entry. A porous bronze tube of length to diameter ratio of about 9·3 was employed for the purpose. The inlet Reynolds number based on tube diameter was varied in steps of approximately 10000 from 11000 to 101000. The fractional mass extraction parameter α, defined as the ratio of mass flow extracted over the entire tube length to the entry mass flow, was varied in steps of 0·1 from zero to unity. Measurements were made of the

static pressure changes along the tube, the axial velocity profiles, and the distribution of the magnitude of the absolute turbulent velocity fluctuation at the exit plane. A traverse of the difference between the local and wall static pressures was also taken in the exit plane.

The first experimental investigation into the velocity and pressure distribution in turbulent pipe flow with uniform suction was carried out by Weissberg and Berman [6, 7]. Axial pressure distribution and profiles of temporal-mean axial velocity and axial turbulent velocity fluctuation were measured with air flowing in a 7·31 m long porous pipe of 76 mm dia. Immediately before entering the test section the air underwent an area reduction of just over 11:1 from a settling chamber, so that the entry velocity profile was virtually flat. The Reynolds number was varied from about 25 000 to 80 000, and the entrance suction coefficient β_1, defined as the ratio of the transverse velocity of the sucked air at the wall to the inlet mean axial velocity, was varied from zero to about 0·005. Turbulence levels over the entire pipe cross-section were found to be lowered by suction. At a given location and at the same Reynolds number, velocity profiles were flatter and friction factors higher with suction than without. However, the changes in the velocity profiles resulting from suction were small enough for the velocity profile parameter δ, defined as the ratio $\overline{u^2}/\bar{u}^2$, to have an almost constant value close to 1·02 for all rates of suction tested.

Wallis [8] performed experiments with air flowing in canvas hoses of about 25 mm diameter and of lengths up to 2·3 m, with the entry velocity profile undeveloped. A Reynolds number range of 25 000–121 000 was covered and in this range the friction factor without suction for the rough canvas hose was constant. The entrance suction coefficient β_1 was varied from zero to 0·02. The suction rate along the tube was fairly uniform, although no attempt was made to control it. Wallis presented his results in terms of pressure changes and did not compute friction factors, but his data suggest that these factors, for a given value of β_1 and x/D, were independent of the inlet Reynolds number Re_{D1}, perhaps owing to the considerable surface roughness. Wallis, when using total extraction, took a single velocity profile roughly half-way down the 2·3 m long tube and observed a more peaky profile than at inlet, in contrast to the flatter profiles found by Weissberg and Berman. No turbulence measurements were taken.

Aureille [9] studied the effect of uniform suction on an initially fully-developed turbulent flow of air in a 75 mm dia. sintered nickel tube. The inlet Reynolds number was fixed at 40 800 for all tests while β_1 was varied from zero to 0·00308. At such low rates of suction the static pressure gradient was found to be constant for $x/D > 6$. Aureille found, unlike Wallis, that the axial velocity profile became flatter with suction. Friction factors increased both with β_1 and with x/D. He noted no change, however, in the distribution of radial velocity with x/D. Aureille also deduced from his experimental data, that turbulence was partially destroyed by suction.

To the best of the present authors' knowledge, no experimental work other than [9] has been reported on the initially fully-developed turbulent flow of air in porous tubes of circular cross-section when uniform suction is applied at the wall. In the present work an extensive range of Reynolds number and a much wider range of the entrance suction coefficient β_1 (from zero to about 0·027) have been covered. Local and average friction factors have been computed, as well as a novel dimensionless wall shear stress expressed in terms of the average axial momentum associated with the extracted air. An empirical correlation for pressure gradients with suction is proposed. The velocity profile has been found to become flatter at modest rates of suction but more peaked at large rates of suction, thus explaining the apparent disagreement that has so far existed. This work, however, does not support the findings of some previous authors that the turbulence level over the entire pipe cross-section is reduced by the presence of suction.

2. SOME GENERAL CONSIDERATIONS

The flow within a tube without suction is fully determined at all points if at inlet to the tube the Reynolds number and the velocity distribution, including the turbulence pattern, are prescribed, and in addition a geometric parameter such as the 'equivalent sand roughness k_s/D, defines the departure from smoothness at the inner surface. It then follows, for example, that the local dimensionless shear stress at the wall surface can be written as a function

$$\frac{\tau_{w0}}{\frac{1}{2}\rho\bar{u}^2} = f_0 = f_0\left(\frac{\rho\bar{u}D}{\mu}, \frac{x}{D}, \frac{k_s}{D}\right). \quad (1)$$

With suction a full description of suction rate along the entire inner wall surface must, in addition, be given, and this must consist of the distribution of the suction velocity from the inlet $x = 0$ to the exit $x = L$. It is clear that with suction a wide variety of boundary conditions is possible, and it is necessary to limit the study to a very narrow range of possibilities.

Firstly it was decided to position the porous section at the end of a long impervious tube of the same diameter so that fully developed turbulent flow would be achieved prior to the porous section at all Reynolds numbers tested.

Secondly, it was decided to study a range of suction when the rate of mass extraction per unit area was uniform over the entire inner surface. Since the experiments covered flow which in all cases could be considered 'incompressible', this also implied a uniform suction velocity v_w normal to the surface, and v_w was expressed in non-dimensional form as $v_w/\bar{u}_1$ and denoted by the symbol β_1. With certain qualifications to be raised later in this section, β_1, in conjunction with the specification of uniform suction, fully determines the wall boundary conditions.

An alternative parameter to β_1 is the fractional mass extraction parameter α, which for the given value of L/D and the assumption of uniform suction can be shown to be equal to

$$\alpha = 1 - \frac{\bar{u}_2}{\bar{u}_1} = 4\beta_1\frac{L}{D}. \quad (2)$$

Another parameter which for uniform suction is equivalent to β_1, is the ratio $\beta = v_w/\bar{u}$, where $\bar{u}$ is the local mean velocity, and β must increase towards the exit of the tube because $\bar{u}$ falls off linearly in the same direction. It can then be shown that

$$\beta = \frac{v_w}{\bar{u}} = \frac{\beta_1}{[1 - \alpha(x/L)]} = \frac{\beta_1}{[1 - 4\beta_1(x/D)]}. \quad (3)$$

Thus it emerges that the local wall shear stress with suction can be expressed in terms of the parameters listed in equation (1), and any one of β_1, α or β.

The above remarks must now be qualified, firstly because the suction cannot be entirely uniform at least at the microscopic level. The inner surface must in practice contain numerous pores resulting in a discontinuous surface, partly permeable and partly solid. This means that for the purpose of discussing the shear stress it is necessary to define carefully what is meant by 'surface'. A cylindrical surface of radius R, where R is the mean radius of the impermeable regions, can be drawn so as to extend over both the permeable as well as the impermeable regions and this will be considered the 'effective surface' of the porous tube (Fig. 1).

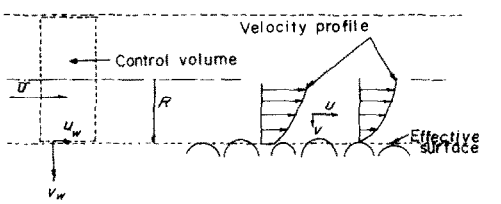

FIG. 1. The flow at the effective surface.

When suction is applied, there must exist in the region of a pore a flow normal to this effective surface. If this flow is considered over a finite area of the effective surface (which will simply be called surface henceforth) containing both pores and impermeable regions, then an effective normal velocity v_w can be defined as the mass flow per unit surface area divided by the density.

A second difficulty arises because the fluid

crossing the surface into the pores may have an axial velocity component at the surface. If the average value of this component for the mass leaving unit area is u_w, then $\rho u_w v_w$ represents the rate at which axial momentum crosses the surface. By considering the conservation of axial momentum of the control volume shown dotted in Fig. 1, it can be shown that the quantity $-\mu(\partial u/\partial r)_w + \rho u_w v_w$ appears in the equation. The first term represents the shear stress acting on the control volume–and therefore the rate of transfer of axial momentum—due to viscosity, whereas the second term represents the rate of depletion from the control volume of the axial momentum associated with the sucked fluid, per unit surface area of the tube. Thus the tube experiences an axial stress equal to $\rho u_w v_w$ in addition to the viscous shear stress. The sum of the two terms will be called the 'effective wall shear stress with suction', viz.

$$\tau_{we} = -\mu\left(\frac{\partial u}{\partial r}\right)_w + \rho u_w v_w \qquad (4)$$

and the corresponding effective friction factor will be defined as

$$f_e = \frac{\tau_{we}}{\frac{1}{2}\rho\bar{u}^2}. \qquad (5)$$

It will be shown in section 4 that the value of the effective wall shear stress can be readily computed from experimental data with the aid of the momentum equation. To separate the two effects appears at present impossible because it requires a knowledge of u_w, and it does not seem possible to measure this in any practical way. A few remarks about u_w are nevertheless appropriate, although these can only be speculative.

Different tubes may have flows in which u_w, and hence $\rho u_w v_w$ and τ_{we}, differ despite the fact that Re_D, x/D, k_s/D and β are the same. Such variation will be due to differences in the structure of the porous surface, and it seems likely that u_w will depend largely upon the proportion of pore to total surface area, viz. A_p/A_s; it will also depend on whether the total pore area consists of a few large pores or many small ones, and it will thus depend on the number of pores per unit surface area. The internal structure of the wall may also have some influence on the direction of the suction velocity: a wall having many radial capillary passages may behave differently from one having numerous interconnecting passages formed by the sintering of metal spheres. It seems likely that the finer the pore structure, the smaller will be the value of u_w. No experiments were carried out to determine the effect of wall structure upon τ_{we}, however, and therefore the results obtained can only be applied with confidence to tubes having a surface structure similar to that tested.

3. APPARATUS AND INSTRUMENTATION

The general arrangement of the apparatus and its associated instrumentation is shown schematically in Fig. 2. Air from a mains supply at about 7 bar was delivered through preliminary filters, regulating valves and an orifice plate to the settling tube of 48 diameters in length, from which the air entered the test section in fully-developed turbulent flow. The porous tube in the test section was surrounded by a housing divided into four chambers of equal axial length, these being sealed against cross leakage between them. Uniformity of suction was controlled independently by a needle valve at the exit of each chamber, while overall control of suction was obtained with a diaphragm valve downstream of the test section which set the average pressure level within the porous tube. One float-type flowmeter measured the total quantity of air extracted through the four chambers, and another measured the air leaving the tube. The exit plane of the porous tube was instrumented so that it could be traversed with static, pitot or hot-wire probes. The various parts of the apparatus are described in further detail below.

3.1 *The porous tube*

The porous tube used in the investigation was supplied by Messrs. Sintered Products Ltd. under the trade name of 'Porosint'. The tube was manufactured by the moulding and sintering of carefully graded spherical particles made by

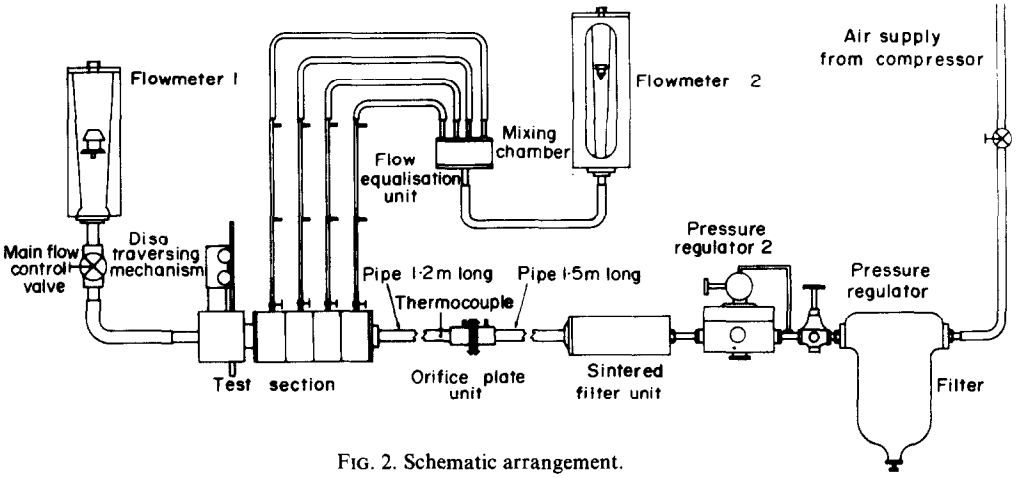

FIG. 2. Schematic arrangement.

an atomisation process from bronze alloy consisting of 89 per cent Cu and 11 per cent Sn. Because it was intended that the extraction rate along the tube be reasonably uniform before final adjustment with the four-chamber control described above, a tube was selected that would have a pressure drop across its porous wall much greater than the pressure change along it. Hence the thickest available tube of the finest grade was chosen (6·3 mm thick, grade A) with a mean particle diameter of 13 μm and a nominal filtration rating of $2\frac{1}{2}$ μm, and having an overall porosity of 26 per cent. The length of the tube was 245·2 mm, and its internal diameter 25·65 mm. Typical extreme conditions occured at an inlet Reynolds number of 101 000 when operating with total extraction. Under these conditions the absolute pressure in the tube was about 3·25 bar, the pressure drop across its wall was about 2 bar, while the pressure difference along it was only 0·006 bar.

The tube, as originally purchased, tapered from 25·4 mm at one end to 25·9 mm at the other. In careful experiments without suction, two methods were used to correct for taper: firstly by calculation using Bernoulli's equation, and secondly by taking the average of the pressure drops when passing the air first one way and then the other through the tube. Good agreement with the Blasius law up to a Reynolds number of 101 000 was achieved by both methods, thereby demonstrating that the tube was hydrodynamically smooth up to that Reynolds number, but because it was not possible to make a reliable correction for the taper under suction conditions, it was decided to machine the bore of the tube. After machining the bore was etched electrolytically to reopen the surface pores. An average i. d. of 26·42 mm with a maximum variation of ± 0·24 per cent was attained, but the etching resulted in a roughening of the surface, with 'Talysurf' readings giving an average value of 0·00142 for the relative roughness k/R. Experiments without suction showed that the friction factors after etching agreed with the Colebrook–White law when using an equivalent sand roughness k_s/R of 0·0015, thus showing that the 'physical' roughness in this case corresponded very nearly to the equivalent sand roughness.

The end flanges that held the porous tube were provided with static pressure tappings, and three

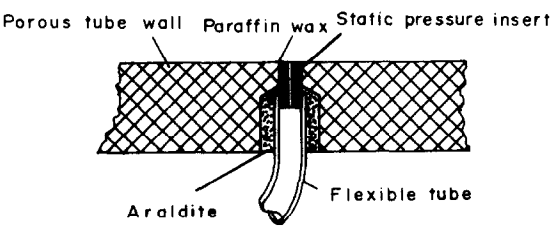

FIG. 3. Static pressure tapping in porous tube.

further tappings were set in the tube such that they divided the total length into four equal sections. Each tapping in the tube wall was formed from a 1·5 mm dia. brass stub having a 0·8 mm dia. central hole (Fig. 3) in such a manner that they were nearly flush with the inner surface but certainly not proud of it. A very small quantity of wax was applied to the porous surface around the inserts, so that the streamlines would run locally parallel to the tube axis.

3.2 *Flow instrumentation*

Each float-type flowmeter was calibrated *in situ* against the orifice plate in the inlet tube to the test section, when running the rig first with no suction, and then with total extraction. The rates of flow from individual chambers were equalised by equalising the frictional pressure drops in four similar copper tubes of 6·2 mm bore. Each of these tubes was calibrated against a positive-displacement gas meter, and the total of their four readings was checked against the orifice plate.

In order to check that the flow at entry to the porous tube under no suction conditions was axi-symmetric and fully developed, velocity profiles at various Reynolds numbers were obtained, using a 1·2 mm o.d. hypodermic T-probe whose stem offered a constant blockage to the flow at all probe positions. The profiles were in good agreement with those obtained by Nikuradse.

The radial distribution of both the temporal-mean axial velocity and the absolute turbulent velocity fluctuation were measured in the exit plane by a calibrated hot-wire probe of the DISA type 55A36, using a DISA 55D01 constant temperature anemometer. The hot wire was so positioned that it was almost equally sensitive to both radial and axial velocity components, but since the temporal-mean radial component was under most test conditions considerably smaller than the corresponding axial component, the effect of the former upon the temporal-mean readings has been ignored, and the values taken to represent axial velocity. The probe was traversed from the axis to within 0·59 mm of the tube inner surface.

A static probe made from 1·2 mm o. d. hypodermic tube was used to measure the distribution of static pressure in the exit plane. The static pressure changes along the tube were measured by a Betz manometer which could be read to 0·01 mm H_2O.

4. REDUCTION OF EXPERIMENTAL DATA

It has been stated that the flow in the tube with suction was considered incompressible. This was justified because the flow was essentially isothermal, the changes in static pressure were only small, and the highest Mach number achieved was less than 0·2.

Measurements of the radial distribution of static pressure over the range of Reynolds number and suction covered by the experiments revealed a negligible variation across the tube, and therefore the static pressure at any section of the tube was assumed to be constant.

With the above assumptions, and considering axi-symmetric turbulent flow, the continuity and x-momentum equations can be expressed as

$$r\frac{\partial u}{\partial x}+\frac{\partial}{\partial r}(rv)=0 \tag{6}$$

$$u\frac{\partial u}{\partial x}+v\frac{\partial u}{\partial r}=-\frac{1}{\rho}\frac{\partial p}{\partial x}+\nu\frac{\partial^2 u}{\partial x^2}+\frac{\nu}{r}\frac{\partial}{\partial r}\left(r\frac{\partial u}{\partial r}\right)+\frac{1}{r}\frac{\partial}{\partial r}(r\overline{u'v'}). \tag{7}$$

Multiplying (7) throughout by r, taking $\partial p/\partial x = \mathrm{d}p/\mathrm{d}x$, and making use of the continuity equation (6), equation (7) can be integrated with respect to r between the limits $r = 0$ and $r = R$, R being the radius of the inner surface of the tube. This integration gives

$$\frac{1}{2\pi\rho}\frac{\partial}{\partial x}(\delta m\bar{u})=-\frac{R^2}{2\rho}\frac{\mathrm{d}p}{\mathrm{d}x}+\frac{\nu}{2\pi\rho}\frac{\partial^2 m}{\partial x^2}-\frac{R}{\rho}(\tau_w+\rho u_w v_w) \tag{8}$$

where δ is the velocity profile parameter

$$\delta = \frac{\overline{u^2}}{\bar{u}^2} = \frac{\int_0^1 (u/u_{max})^2 \bar{r}\, d\bar{r}}{2\left[\int_0^1 (u/u_{max})\bar{r}\, d\bar{r}\right]^2} \quad (9)$$

m is the rate of axial mass flow

$$m = \rho\bar{u}(\pi R^2) \quad (10)$$

and τ_w is the viscous wall shear stress

$$\tau_w = -\mu\left(\frac{\partial u}{\partial r}\right)_w. \quad (11)$$

Here u_w and v_w are respectively the temporal mean axial and radial velocities at the tube inner surface. For the case of uniform suction, v_w and $(\partial m/\partial x)$ are both constant. Equation (8) can then be simplified, by introducing the effective shear stress from equation (4), to

$$\frac{\partial}{\partial x}(\delta m\bar{u}) = -\pi R^2 \frac{dp}{dx} - 2\pi R\tau_{we}. \quad (12)$$

4.1 *Local effective friction factors with suction*

Integrating the continuity equation (6) between $r = 0$ and $r = R$, one obtains

$$\frac{\partial\bar{u}}{\partial\bar{x}} = -2v_w\left(\frac{L}{R}\right). \quad (13)$$

Using the definition of equation (5), equation (12) can be reduced to give

$$f_e = -\frac{1}{2(1-\alpha\bar{x})^2}\frac{\partial\Pi}{\partial\bar{x}} + 4\delta\beta - \frac{R}{L}\frac{d\delta}{d\bar{x}} \quad (14)$$

where $\bar{x} = x/L$ is the dimensionless axial distance, and Π is a pressure coefficient defined by

$$\Pi = \frac{p - p_1}{\frac{1}{2}\rho\bar{u}_1^2}\frac{R}{L}. \quad (15)$$

Π was calculated from measured values of static pressure along the porous tube, using equation (15). Least squares second order curves were fitted to the values of Π and differentiated to give values of $(\partial\Pi/\partial\bar{x})$. The local suction coefficient β was obtained from equation (3). With suction, velocity profiles were measured only at the outlet of the porous tube, and values of δ at other values of $\bar{x}$ could not be obtained. However, for fully developed turbulent flow, as it existed at inlet to the porous tube, δ was verified to be about 1·02 in the Reynolds number range covered, and it was assumed that suction along the tube did not alter the profile at entry from that attained under no suction conditions. It was found that at outlet, values of δ varied from 1·01 to 1·11, depending on the intensity of suction (see Fig. 7). If it is assumed that δ varies steadily and without steep changes between the inlet and outlet values, δ_1 and δ_2, then it can be shown that the term involving $d\delta/d\bar{x}$ in equation (14) is much smaller than the other two terms on the right-hand-side of the equation. It was therefore considered satisfactory, in view of the small variation of δ, to assume that δ varied linearly with $\bar{x}$ between sections 1 and 2. Hence it follows that

$$\frac{d\delta}{d\bar{x}} = \delta_2 - \delta_1 \quad (16)$$

and

$$\delta = \delta_1 + (\delta_2 - \delta_1)\bar{x} \quad (17)$$

with δ_1 taken as 1·02. Values of δ_2 plotted in Fig. 7 were calculated from equation (9). Each velocity profile was integrated, using Simpson's rule to evaluate δ.

4.2 *Average effective friction factors with suction*

The average value of the effective friction factor, $\bar{f}_e$, over the tube length x can be defined as

$$\bar{f}_e = \frac{\bar{\tau}_{we}}{\frac{1}{2}\rho\bar{u}_1^2} = \frac{1}{\frac{1}{2}\rho\bar{u}_1^2\bar{x}}\int_0^{\bar{x}} \tau_{we}\, d\bar{x}. \quad (18)$$

Integrating equation (12) with respect to $\bar{x}$ between the limits $\bar{x} = 0$ and $\bar{x}$, one obtains

$$\bar{f}_e = -\frac{\Pi}{2\bar{x}} + \frac{R}{L\bar{x}}\left[\delta_1 - \delta(1-\alpha\bar{x})^2\right]. \quad (19)$$

Equation (19) was used to compute average effective friction factors over lengths varying in

steps of $\Delta(x/D) = 1$, from $x/D = 1$ to $x/D = 9$. At $x/D = 0$ equation (19) becomes indeterminate, but at the entry section the average value coincides with the local value of the effective friction factor as calculated from equation (14).

The analysis of this section may be taken to imply that at $x/D = 0$ there must exist a discontinuity in the value of the shear stress from that obtained in fully developed turbulent flow without suction, to the value obtained from equation (14). In practice, no doubt, the velocity profile immediately upstream of the entry section to the porous tube will depart somewhat from the fully developed shape, and there will be a gradual transition from the no-suction to the suction value of the shear stress.

5. EXPERIMENTAL RESULTS

5.1 *Results without suction*

Before the apparatus could qualify for experiments with suction, it was necessary to prove that the apparatus would produce acceptable results without suction. When measured values of pressure coefficient without suction were plotted against x/D, they showed an acceptably low degree of scatter, particularly in view of the difficulties associated with putting pressure tappings into a porous wall. Friction factors without suction, f_0, were calculated, from the least squares straight lines fitted to the values of the pressure coefficients, for a range of Reynolds numbers. These are seen plotted against Re_D in Fig. 4. Also plotted on the same graph are friction factors for a hydraulically smooth tube as computed from the Blasius friction law

$$f_0 = \frac{0{\cdot}0791}{(Re_D)^{0{\cdot}25}} \tag{20}$$

and friction factors for a rough tube as computed from the Colebrook–White semi-empirical relation

$$\frac{1}{f_0^{\frac{1}{2}}} = 3{\cdot}48 - 4\log\left[\frac{k_s}{R} + \frac{9{\cdot}35}{(Re_D)f_0^{\frac{1}{2}}}\right] \tag{21}$$

taking the roughness parameter $k_s/R = 0{\cdot}0015$. The experimental points are in good agreement with the latter equation and this value of the roughness parameter is very close to the measured value indicated in section 3.1.

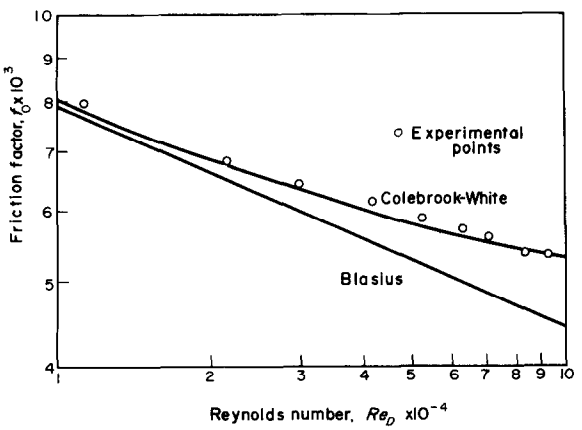

FIG. 4. No-suction friction factors.

5.2 *Results with suction*

Measurements of pressure gradient. For a typical value of the inlet Reynolds number Re_{D1}, pressure coefficients based on inlet dynamic head are shown plotted against x/D for various values of the entrance suction coefficient β_1 (Fig. 5). Save for very low rates of suction, pressure rises rather than falls are generally registered in the direction of flow. This is because the rate of loss of momentum of the fluid resulting from suction more than overcomes the wall friction. At high rates of suction, the rate of rise of pressure coefficient is rapid at the entrance of the tube, falling somewhat as the end is approached, and the reverse applies at low rates of suction.

For given inlet Reynolds numbers, best values of K_1 to K_6 for the following correlation have been computed, using the method of least squares applied to the experimental data:

$$\frac{p - p_1}{\frac{1}{2}\rho\bar{u}_1^2} = \frac{4x}{D}\left[K_1 + K_2\beta_1 + K_3\beta_1^2 + \frac{x}{D}\beta_1(K_4 + K_5\beta_1 + K_6\beta_1^2)\right]. \tag{22}$$

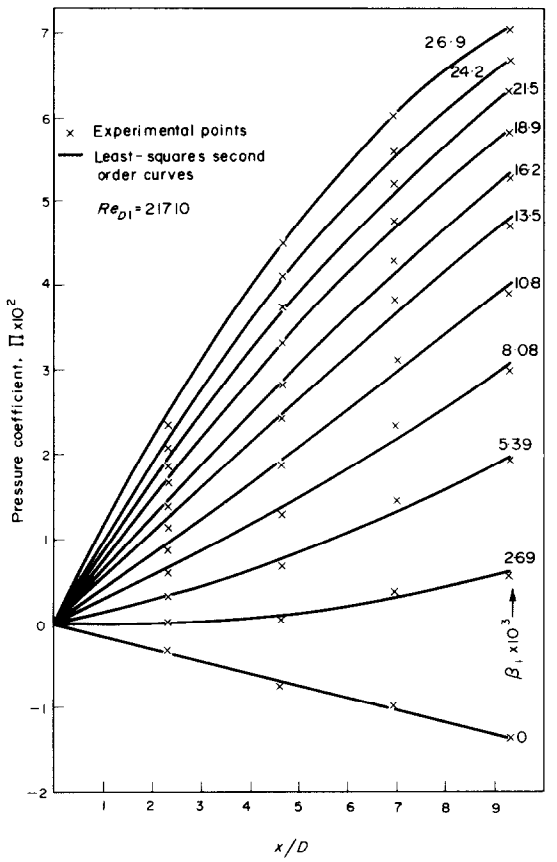

FIG. 5. Variation of pressure coefficient with suction.

In the case of no suction β_1 is zero, so that (22) reduces to

$$\frac{p - p_1}{\frac{1}{2}\rho \bar{u}_1^2} = \frac{4x}{D} K_1 \qquad (23)$$

where K_1 is the no-suction friction factor corresponding to the inlet Reynolds number. The coefficients K_1 to K_6 are functions of the inlet Reynolds number alone, and their values are given in Table 1.

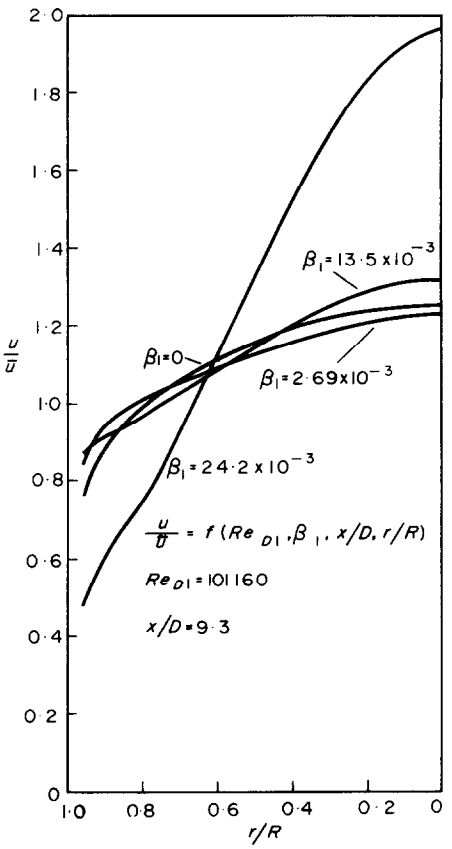

FIG. 6. Non-dimensional velocity profiles.

Table 1

Re_{D1}	K_1	K_2	K_3	K_4	K_5	K_6
11260	−0·007968	2·154	8·654	0·2081	−17·05	241·5
21710	−0·006855	2·448	−7·287	0·1444	−14·43	236·4
29980	−0·006434	2·557	−10·96	0·1089	−11·54	171·7
41840	−0·006154	2·709	−12·42	0·1573	−17·79	330·9
52120	−0·005886	2·773	−14·77	0·1576	−18·92	372·4
62550	−0·005745	2·600	−8·982	0·1596	−18·90	369·4
70670	−0·005616	2·954	−20·87	0·1286	−17·40	353·2
83280	−0·005391	3·135	−30·46	0·0707	−12·25	241·8
91420	−0·005350	3·469	−42·48	0·0386	−10·47	218·0
101160	−0·005249	3·512	−44·16	0·0308	−10·02	213·9

Profiles of axial velocity. In Fig. 6 non-dimensional distributions of axial velocity in the exit plane, with an inlet Reynolds number Re_{D1} of 101 160 and at three different values of the inlet suction coefficient β_1, are compared with the corresponding distribution for fully developed turbulent flow without suction. The velocity profile in the core of the flow becomes slightly more peaked at low rates of suction but markedly so at higher rates. This effect is principally caused by diffusion, a similar effect being found in divergent channels [10]. In the immediate vicinity of the wall, where the slow-moving air is being sucked away, the velocity gradients increase continuously with suction as evidenced by the increased wall shear stress, although it was not possible to make velocity measurements in this region. It is interesting to note that at very low rates of suction the non-dimensional velocity, $u/\bar{u}$, near the wall becomes greater than the corresponding no-suction value, giving rise to a flattening of the profile in this region, as the area of faster moving fluid enlarges to fill more of the tube.

When the ratio of the velocity profile parameter at exit, δ_2, to the same quantity at entry, δ_1, was plotted against β_1 for various Reynolds numbers, the experimental points were scattered about a fairly well defined curve, with no consistent variation due to Reynolds number appearing. Since the effect of the change of δ, viz. $d\delta/d\bar{x}$, upon the friction factor has been assumed to be small, it was considered sufficiently accurate to use values established from the least squares third order curve that fitted the average values of δ_2/δ_1 over the experimental range of Reynolds number at each suction rate (Fig. 7). This curve can be represented by the equation

$$\frac{\delta_2}{\delta_1} = 1 - 0{\cdot}105\,\beta_1 - 232\,\beta_1^2 + 16\,113\,\beta_1^3. \quad (24)$$

Figure 7 shows clearly that the net effect of suction is to make the velocity profile fuller at modest suction, and to make it more peaked as the suction rate becomes greater. Weissburg [6] and Aureille [9] also found that velocity profiles became fuller at low rates of suction, and Wallis [8] found a peaked profile at higher suction. Although the range of suction coefficient covered by the present experiments included all those used by other investigators, no precise comparison between profiles can be made because of differing flow conditions.

Effective wall shear stress with suction. The effective wall shear stress for the full range of Reynolds number was calculated from the pressure coefficients and values of δ, using equation (14), and the variation of this stress along the tube at various suction rates and at a fixed inlet Reynolds number of 21 710 is shown in Fig. 8. τ_{we} is normalized with respect to the no-suction shear stress, τ_{w0}, given by $f_{01} \times \frac{1}{2}\rho\bar{u}_1^2$

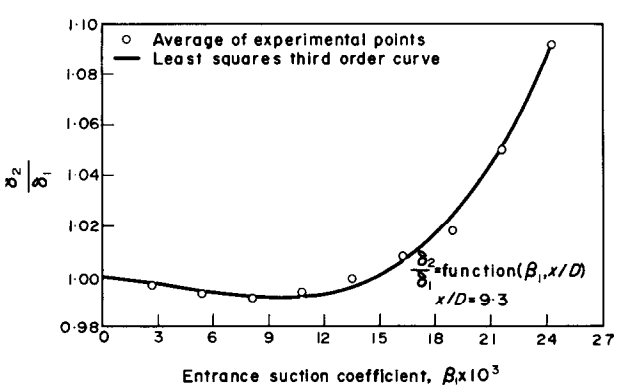

FIG. 7. Velocity profile parameter vs. entrance suction coefficient.

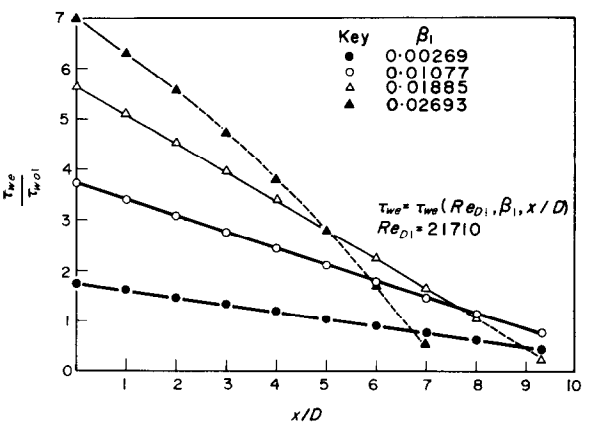

FIG. 8. Variation of effective shear stress along the tube.

where f_{01} is the experimentally determined no-suction friction factor corresponding to the inlet Reynolds number and $\frac{1}{2}\rho\bar{u}_1^2$ is the inlet dynamic head that existed under suction conditions.

It will be noticed that the effective shear stress decreases approximately linearly along the tube. If, say, the Blasius law were to apply, a decrease with $(1 - \alpha\bar{x})^{\frac{1}{4}}$ could have been expected, because according to this law the shear stress is proportional to $\bar{u}^{\frac{1}{4}}$, while with uniform suction $\bar{u}$ falls off linearly with $\bar{x}$. It is difficult to explain the linear variation simply, because it is the result of several factors varying simultaneously: a falling local Reynolds number, a rising local suction coefficient β, and a continuously changing velocity profile along the tube. What is certain is that suction increases the stress well above the value that can be expected from a Blasius-type law.

At very high suction rates, negative values of effective shear stress were obtained at large values of x/D. These particular results are open to some doubt and are therefore not being shown here. When all the air is sucked away, however, negative values of the effective wall shear stress near the exit plane of the tube are conceivable, resulting from end effects at the closed end of the tube. The flow in the inner region just upstream of the closed end may reverse direction, and this would result in the negative wall shear stress, even though the bulk of the fluid at the same cross-section may still suffer positive shear by virtue of its positive direction of flow.

At a given value of x/D, τ_{we} generally increases with β_1, this increase being more pronounced at low suction rates and towards the tube entrance.

Local effective friction factors. The values of local effective friction factors with suction have been divided by the no-suction friction factors computed from the Colebrook–White friction law at the same local Reynolds number as existed with suction, and they have been plotted for two representative inlet Reynolds numbers of 21 700 and 83 280 in Figs. 9 and 10 in the form of carpets where x/D and β_1 are the two floating variables. This ratio, f_e/f_{CW}, therefore takes into account the effect of the changing Reynolds number along the tube. At large values of β_1 and especially at the lower Reynolds numbers, f_e/f_{CW} falls markedly towards the end of the tube. Under these conditions, however, the computation of f_e is unreliable because the first and second terms on the right-hand side of equation (14) are of the same order of magnitude and of opposite sign (the third term always being very small). Eventually f_e becomes negative, this being almost certainly due to the end effects mentioned earlier; the negative values are not shown because they are not considered reliable.

It is likely that the ratio f_e/f_{CW} depends upon local quantities, namely the local Reynolds number, Re_D, the local suction coefficient, β, and the location in the tube, x/D, Appropriate local values have therefore been extracted from the

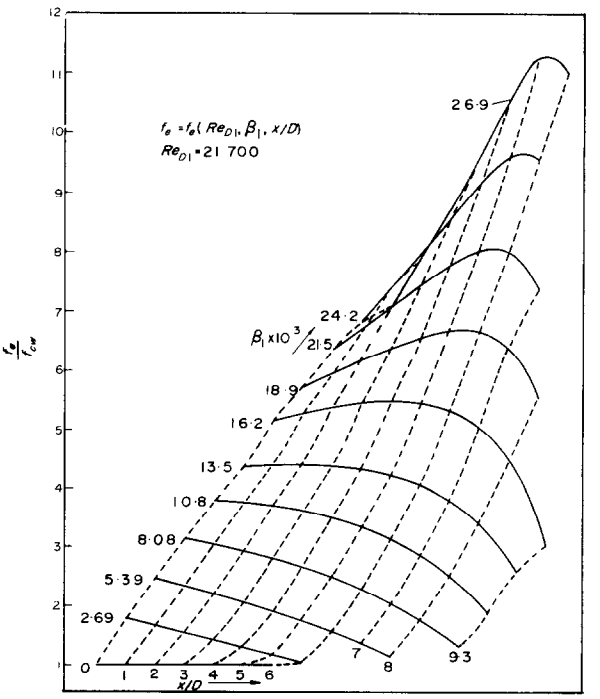

FIG. 9. Local effective friction factors with suction.

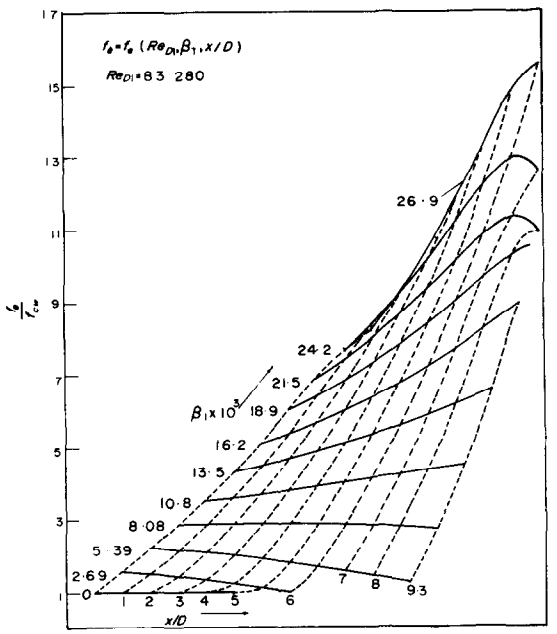

FIG. 10. Local effective friction factors with suction.

experimental data by interpolation based on least-squares curve fits. The results are shown in Figs. 11–13, where f_e/f_{cw} is seen plotted against β for various values of x/D at three different Reynolds numbers. At a fixed Reynolds number, friction factors always increase with the suction coefficient, the rate of rise generally being greater at higher values of β. For a given suction coefficient, friction factors fall with x/D, their dependence on x/D being very much less at the higher Reynolds numbers. With all other variables remaining fixed, f_e/f_{cw} is generally higher at larger values of Re_D, but insufficient data were available to establish a relation.

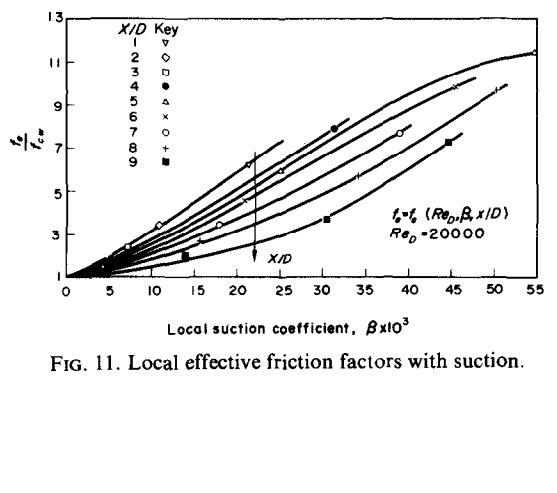

FIG. 11. Local effective friction factors with suction.

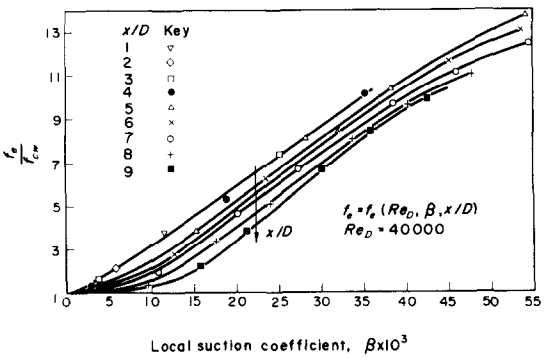

FIG. 12. Local effective friction factors with suction.

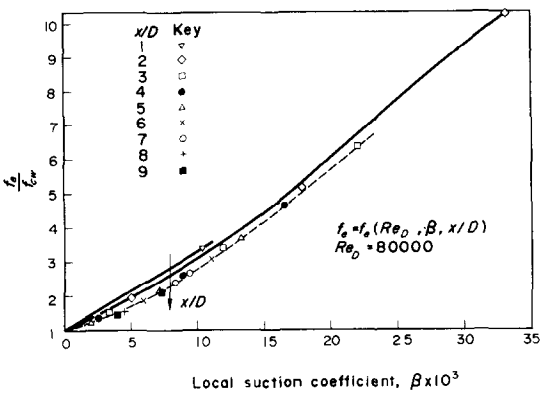

FIG. 13. Local effective friction factors with suction.

Effective wall shear stress and momentum loss. When a condensing vapour flows parallel to a condensate film, the vapour will exert a shear force on the liquid–vapour interface which can be considered analogous to the force exerted on a porous wall with high rates of suction. Several authors have suggested, explicitly or implicitly, that the shear stress under such conditions is of a magnitude between 0·5 $\rho\bar{u}v_w$ and 1·0 $\rho\bar{u}v_w$, where ρv_w represents the rate of condensation per unit area of interface, and $\bar{u}$ is the average vapour velocity relative to the interface.

To test the validity of this assumption, it suggests itself that the effective shear stress τ_{we} in equation (5) should be normalized by dividing τ_{we} by $\rho\bar{u}v_w$ instead of by $\frac{1}{2}\rho\bar{u}^2$. $\rho\bar{u}v_w$ can be taken to represent the average axial momentum possessed by the mass extracted per unit surface area. If the assumption is correct, results should yield values of the ratio $\tau_{we}/\rho\bar{u}v_w$ between 0·5 and 1·0, thereby also suggesting that suction is the main influence on the magnitude of wall shear stress under such conditions. Indeed, if the profile parameter δ were constant along the tube and equal to unity, as it would be in slug flow, a value of 1·0 could be expected; in fact δ was about 1·02 at entry and it was varying along x/D.

The disadvantage of normalizing τ_{we} with $\rho\bar{u}v_w$, however, is that at zero suction the normalized value of τ_{we} becomes infinite. To overcome this difficulty, values were plotted in Fig. 14 normalized by the sum of the corresponding 'no-suction' stress τ_{w0} and the term $\rho\bar{u}v_w$. At low suction rates, the term τ_{w0} $(=f_{CW}\frac{1}{2}\rho\bar{u}^2)$ in the denominator predominates, while at high suction rates it becomes insignificant compared with the $\rho\bar{u}v_w$ term. Figure 14 gives local values

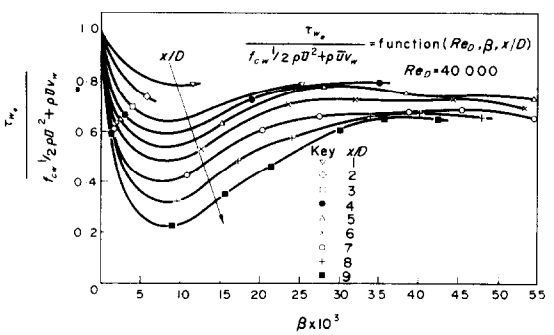

FIG. 14. Local non-dimensional effective shear stress.

of the normalized stress plotted against the local value of β for different locations, x/D, all for a typical value of local Reynolds number of 40 000. Similar curves are obtained at other Reynolds numbers, and in all cases at high values of β the curves bunch together around a value of about 0·7. This suggests that at high rates of suction the effective wall shear stress is about 0·7 of the rate of loss of axial momentum of the sucked fluid, $\rho\bar{u}v_w$, rather than 0·5 as suggested by the Silver and Wallis Reynolds flux model [8]. This factor should, however, be applied with some caution since suction is never uniform under condensation conditions.

These results suggest that at high values of suction, of the three parameters Re_D, x/D, $\rho\bar{u}v_w$, the last appears to be the only significant one affecting the shear stress, and it is tempting to speculate whether roughness—not investigated in the present experiments—might also play an insignificant role.

Average effective friction factors. The graphs of average effective friction factor with suction for two typical Reynolds numbers of 21 700 and 83 280 are presented in Figs. 15 and 16 respectively in the form of a carpet in which the effects of the variables x/D and β_1 is depicted. These plots could be useful to, for instance, a designer who wants to know the power requirements in a similar flow situation. The values of $\bar{f}_e$ have been divided by f_{01} which is the no-suction experimental value of friction factor at the same inlet Reynolds number. $\bar{f}_e$ is seen to be substantially greater than f_{01} for all rates of suction, although it decreases with x/D at all rates of suction. This is because the magnitude of the pressure gradient term in equation (14), containing the local dynamic head in its denominator, is increasing along the tube faster than the momentum term; these two quantities are generally of opposite sign but are of comparable magnitude towards the exit of the tube. The ratio $\bar{f}_e/f_{01}$ is seen to increase with entry Reynolds number, a trend that was confirmed at other values of Re_{D1}.

Turbulence intensity profiles. The distribution of the *relative* turbulence intensity taken in the exit plane at three different suction rates, when the inlet Reynolds number was kept fixed at 101 160, is shown in Fig. 17 together with the no-suction distribution. In the inner region, turbulence intensity decreases at very low suction

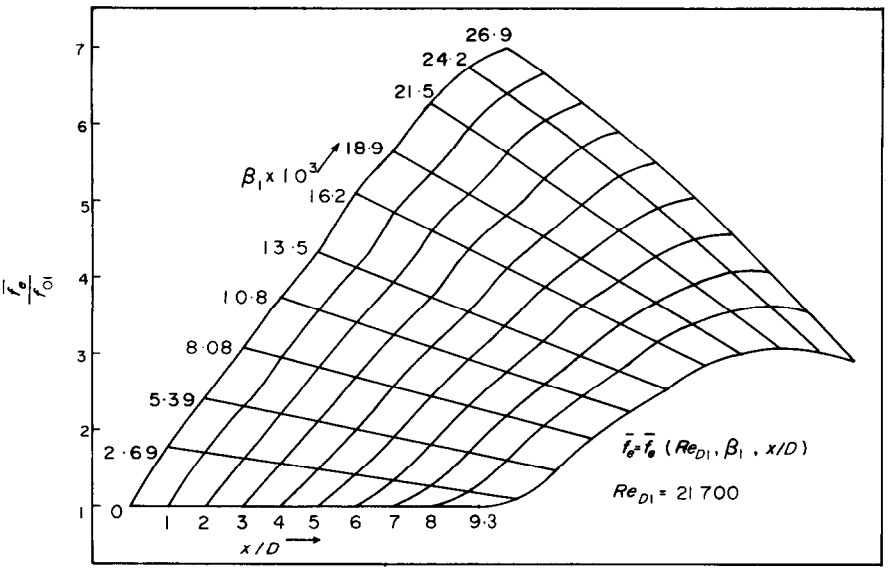

FIG. 15. Average effective friction factors with suction.

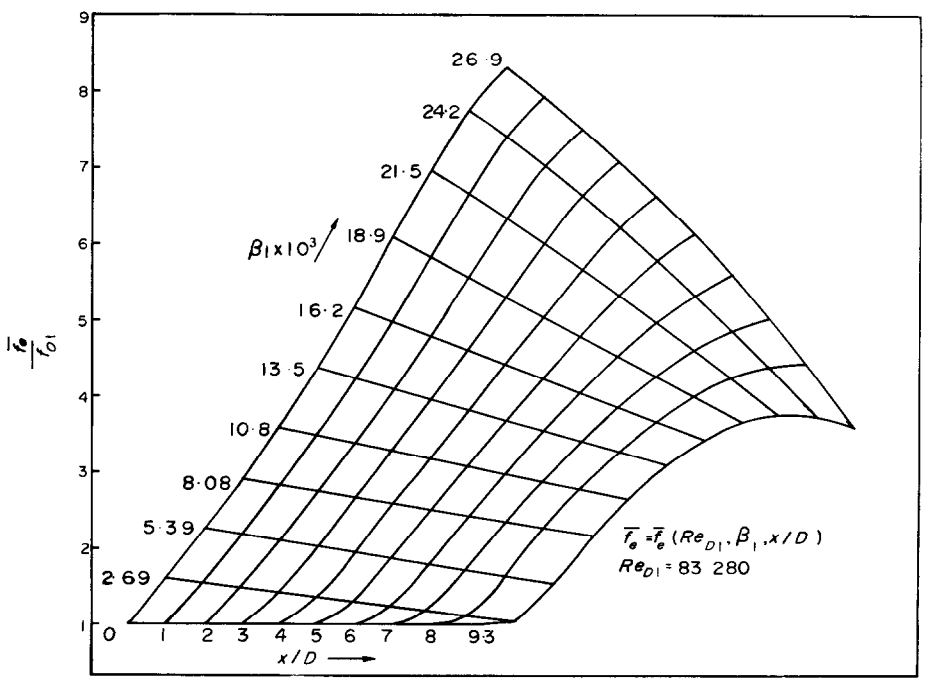

FIG. 16. Average effective friction factors with suction.

rates but increases at higher suction rates; in the core, turbulence intensity is always found to increase with suction. This results firstly in the fully-developed turbulence profile becoming flatter due to suction and secondly developing a maximum (in addition to the one which will exist in the immediate vicinity of the wall) the position of which slowly shifts towards the axis when higher suction rates are applied. These findings are not entirely in agreement with those of Weissberg [6], who measured lower relative turbulence intensities over the entire tube cross-section. However, his suction rates were extremely small, his inlet velocity profile was not fully developed, and it was the exit rather than the inlet Reynolds number that was kept fixed.

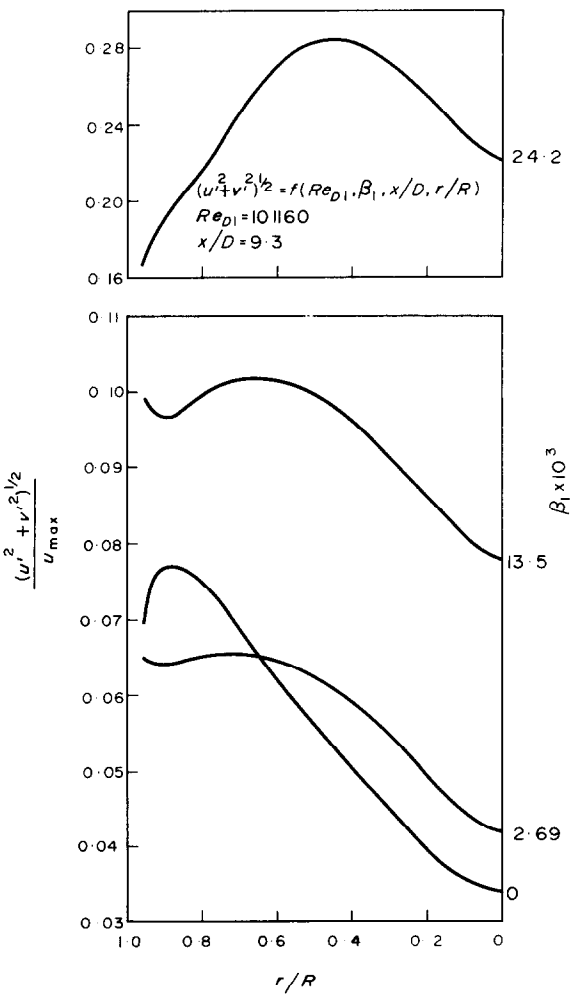

FIG. 17. Relative turbulence intensity profiles.

In the inner (wall) region, reduction in relative turbulence intensity at very low rates of suction is only to be expected because the very highly turbulent fluid existing near the wall under the fully-developed pipe flow condition at entry is now being constantly sucked away. It appears that the increase in turbulence intensity in this region at higher suction rates is associated with the increase in shear stress near the wall under suction. Comparison with the mean velocity profile (Fig. 6) shows that the increase in the velocity gradient is followed by an increase in the turbulence level at the same location, and vice versa.

The data indicate that the magnitude of the *absolute* turbulent velocity fluctuation at the axis stays constant at all suction rates. At no radius does the absolute turbulent velocity fluctuation ever exceed its value with no suction.

6. CONCLUSIONS

Measurements of static pressure and velocity were obtained on an initially fully-developed turbulent flow of air in a porous tube subjected to uniform suction. The axial gradient of pressure coefficient and the velocity profile parameter were calculated from the measured quantities for a range of entrance suction coefficient β_1, and these in turn led to the evaluation of local and average effective friction factors as functions of a suction parameter and location along the tube.

(1) Pressure coefficients with suction, based on the inlet dynamic head, are positive and show a steady rise both with the entrance suction coefficient and x/D, save for very low rates of suction where negative values occur. In the radial direction suction creates a definite, but insignificant, gradient of static pressure.

(2) Except when both β_1 and x/D are very large, the local effective friction factor with suction,

f_e, is higher than the corresponding no-suction value. f_e increases with the entrance suction coefficient. It also increases with x/D at large suction rates, but decreases with x/D at low suction rates.

(3) The local effective friction factor shows an increase with the local suction coefficient β, this increase being somewhat greater at higher Reynolds numbers; at any given value of β it shows a decrease with x/D, although at high Reynolds numbers this dependence is negligible when $x/D > 3$.

(4) The difference between the effective wall shear stress with suction and the corresponding stress without suction is less than the rate of loss of axial momentum that can be associated with the fluid sucked away per unit area, even at very high suction rates. That it is less may be due to the change in radial distribution of axial velocity along the tube, and also perhaps due to the sucked air entering the effective surface with an axial component of velocity u_w. The magnitude of the latter will depend upon the structure of the porous surface, and further work is needed to clarify this point.

(5) The average effective friction factor with suction, $\overline{f}_e$, up to any given location in the tube, is always greater than the no-suction value at the same inlet Reynolds number. $\overline{f}_e$ increases with the entrance suction coefficient but decreases with x/D, this decrease being linear except at very high suction rates.

(6) The profile of axial velocity in the core of the tube always exhibits a peakier shape with suction, an effect similar to that obtained in divergent ducts. The inner (wall) region, comprising the highly curved part of the profile, reduces in thickness with suction.

(7) The relative turbulence level in the wall region is reduced at low suction rates, but at higher suction rates it increases with suction. Within the core of the flow, it always increases with suction.

ACKNOWLEDGEMENTS

The authors would like to thank Dr B. L. Hunt of the Department of Aeronautical Engineering, University of Bristol, for many useful discussions held with him.

REFERENCES

1. F. J. BAYLEY and A. B. TURNER, The transpiration-cooled gas turbine, The University of Sussex Report No. 69/ME/13(1969).
2. F. J. BAYLEY and A. B. TURNER, The heat transfer performance of porous gas turbine blades, *Aeronaut. J.* **72**, 1087–1094 (1968).
3. F. J. BAYLEY and G. R. WOOD, Aerodynamic performance of porous gas turbine blades, *Aeronaut. J.* **73**, 789–796 (1969).
4. P. DUWEZ and H. L. WHEELER, JR., Experimental study of cooling by injection of a fluid through a porous material, *J. Inst. Aero. Sci.* **15**, 509–521 (1948).
5. H. L. WHEELER and P. DUWEZ, Heat transfer through sweat-cooled porous tubes, *Jet Propulsion* **55**, 519–524 (1955).
6. H. L. WEISSBERG and A. S. BERMAN, Velocity and pressure distributions in turbulent pipe flow with uniform wall suction, 1955 Heat Transfer and Fluid Mech. Inst., University of California, Los Angeles, Vol. 14, 1–30. (June 1955).
7. H. L. WEISSBERG, Velocity profiles and friction factors for turbulent pipe flow with uniform wall suction, Union Carbide Nuclear Co., U.S.A. Report K-1264 (April 1956).
8. G. B. WALLIS, Pressure gradients for air flowing along porous tubes with uniform extraction at the walls, *Proc. Instn Mech. Engrs* **180**, 27–35 (1965–6).
9. R. AUREILLE, Contribution à l'étude de l'écoulement turbulent dans une conduite cylindrique poreuse avec aspiration, Publs. scient. tech. Minist. Air No. 433 (1967).
10. S. GOLDSTEIN, *Modern Developments in Fluid Dynamics*, Vol. II, p. 371. Dover, New York (1965).

FACTEURS EXPERIMENTAUX DE FROTTEMENT POUR UN ECOULEMENT TURBULENT DANS UN TUBE POREUX AVEC SUCCION

Résumé—Des mesures de gradient de pression ont été obtenues pour de l'air s'écoulant dans un tube poreux de section droite circulaire avec un profil turbulent entièrement développé à l'entrée et avec une extraction massique uniforme à travers la paroi; on propose une relation empirique pour les gradients axiaux avec succion. Un léger mais insignifiant gradient a été détecté dans la direction radiale. Les expériences couvrent le domaine 11 000–101 000 pour le nombre de Reynolds à l'entrée, avec un rapport

de la vitesse transversale pariétale à la vitesse moyenne axiale à l'entrée variant de 0 à 0,027. Les distributions radiales de la vitesse axiale moyenne dans le temps et de la fluctuation de vitesse turbulente absolue ont été mesurées à la sortie du tube et le paramètre de profil de vitesse a été relié à un paramètre de succion. On trouve que la forme du profil de vitesse moyenne dans le temps dépend de façon critique du taux de succion, devenant plus plate à des taux modestes mais plus pointue à des taux élevés. Le niveau de turbulence relative croît avec la succion pour tous les rayons, mis à part une réduction au voisinage de la paroi à des taux de succion très faibles.

Des valeurs locales et moyennes du facteur de frottement effectif avec succion ont été calculées et sont présentées sous forme graphique. Pour un nombre de Reynolds à l'entrée donné, les valeurs moyennes croissent de façon marquée avec la succion mais décroissent le long du tube. Pour un nombre de Reynolds local donné, les valeurs locales évoluent de la même façon.

EXPERIMENTELL ERMITTELTE REIBUNGSBEIWERTE FÜR TURBULENTE STRÖMUNG MIT ABSAUGUNG IN EINEM PORÖSEN ROHR

Zusammenfassung—Es wurden Messungen des Druckgradienten gemacht mit Luftströmung in einem porösen Rohr mit Kreisquerschnitt bei voll entwickeltem turbulentem Strömungsprofil am Eintritt und bei gleichbleibendem Massenentzug durch die Wand. Es wird eine empirische Beziehung für die axialen Gradienten mit Absaugung gegeben. In radialer Richtung tritt ein kleiner, jedoch unbedeutender Gradient auf. Die Versuche überdecken einen Bereich der Reynoldszahlen am Eintritt von 1000 bis 101000, wobei das Verhältnis Quergeschwindigkeit an der Wand zur grössten Längsgeschwindigkeit am Eintritt zwischen 0 und 0,027 liegt. Die Radialverteilungen der absoluten turbulenten Strömungsgeschwindigkeit wurde am Rohrende gemessen. Der Parameter für das Geschwindigkeitsprofil wurde auf einen Saugparameter bezogen. Das Profil der über die Zeit gemittelten Geschwindigkeit hängt stark vom Saugverhältnis ab. Es verläuft flacher bei mässigen, jedoch steiler bei höheren Saugverhältnissen.

Die relative Turbulenzebene steigt mit dem Sog auf allen Radien an mit Ausnahme einer Abnahme in Wandnähe bei sehr niedrigen Saugverhältnissen.

Örtliche und mittlere effektive Reibungsfaktoren bei Absaugung wurden berechnet und graphisch dargestellt. Bei einer festen Reynoldszahl steigen die Mittelwerte deutlich an, nehmen aber entlang der Rohrlänge wieder ab. Bei einer gegebenen lokalen Reynoldszahl zeigen die lokalen Werte einen ähnlichen Verlauf.

ЭКСПЕРИМЕНТАЛЬНЫЕ ЗНАЧЕНИЯ КОЭФФИЦИЕНТОВ ТРЕНИЯ ПРИ ТУРБУЛЕНТНОМ ТЕЧЕНИИ В ПОРИСТОЙ ТРУБЕ ПРИ НАЛИЧИИ ОТСОСА

Аннотация—Измерены градиенты давления при течении воздуха в пористой трубе кольцевого сечения при полностью развитом профиле турбулентности на входе и при равномерном отсосе массы через стенку. Предложена эмпирическая корреляция для продольных градиентов при наличии отсоса. Отмечен небольшой по величине градиент в радиальном направлении. Опыты охватывали диалазон значений критерия Рейнольдса на входе от $1{,}1 \cdot 10^4$ до $101 \cdot 10^4$ при отношении поперечной скорости отсоса на стенке к средней осевой скорости на входе от 0 до примерно 0,027. Радиальные распределения средней во времени осевой скорости и абсолютной пульсации турбулентной скорости измерялись на выходе из трубы, и проводилась корреляция параметра профиля скорости с параметром отсоса. Найдено, что профиль средней по времени скорости сильно зависит от скорости отсоса, становясь более пологим при умеренных скоростях отсоса и более ррутым при высоких скоростях. Кроме того, относительная степень турбулентности возрастает с увеличением отсоса для радиусов; в пристеночной зоне при очень низких скоростях отсоса отмечено некоторое его ослабление.

Расчитаны и представлены в графическом виде локальные и средние значения эффективного коэффициента трения при отсосе. При постоянном значении критерия Рейнольдса на входе средние значения с отсосом заметно увеличивались, но снижались вдоль трубы. Для данного локального значения критерия Рейнольдса наблюдалась аналогичная тенденция и у локальных значений.